

Electronic Supplementary Information (ESI)

Journal of Materials Chemistry

Liquid Crystalline Octaalkoxycarbonyl Phthalocyanines: Design, Synthesis, Electronic Structure, Self-aggregation and Mesomorphism

Sergey Sergeyev,^a Eric Pouzet,^a Olivier Debever,^a Jeremy Levin,^a Johannes Gierschner,^b Jérôme Cornil,^b Rafael Gómez Aspe^c and Yves Henri Geerts*^a

Synthesis and characterization of **1a,b,d,e**, **2**, **3**

2,3,9,10,16,17,23,24-Octakis(octyl-1-oxycarbonyl)-(29H, 31H)-phthalocyanine (1a).

Prepared similarly to **1c** from **3** (200 mg, 0.23 mmol) and 1-octanol (**4a**) (4 mmol, 0.63 cm³) with the following amendment: flash chromatography (SiO₂, CH₂Cl₂/AcOEt 20 : 1) provided analytically pure product and further purification was not necessary. Green solid. Yield 260 mg (64%). λ_{\max} (CHCl₃)/nm 350 ($\epsilon/\text{dm}^3 \text{ mol}^{-1} \text{ cm}^{-1}$ 85 600), 648 (55 700), 668 (172 000), 705 (179 000); δ_{H} (300 MHz, 0.01 mol dm⁻³ in CDCl₃, Me₄Si, 25 °C) 9.67 (8 H, s, arom. H), 4.67 (16 H, t, *J* 7.0, CH₂O), 2.03 (16H, quint, *J* 7.0, CH₂CH₂O), 1.30–1.70 (80 H, m, CH₂), 0.91 (24 H, t, *J* 6.9, Me), –1.20 (2 H, br s, NH); δ_{C} (75 MHz, 0.01 mol dm⁻³ in CDCl₃, Me₄Si, 25 °C) 167.6, 137.4, 134.5, 124.7, 66.7, 31.9, 29.4, 29.3, 28.8, 26.1, 22.7, 14.1; *m/z* (MALDI) 1763.1 (M⁺).

2,3,9,10,16,17,23,24-Octakis(dodecyl-1-oxycarbonyl)-(29H, 31H)-phthalocyanine (1b).

Prepared similarly to **1c** from **3** (433 mg, 0.5 mmol) and 1-dodecanol (**4b**) (10 mmol, 1.86 g) with the following amendment: the crude product was isolated by flash chromatography (SiO₂, CH₂Cl₂/AcOEt 50 : 1). Then it was dissolved in hexane (50 cm³), and MeOH was added until precipitation of **1b** was complete and the supernatant was nearly colorless. The supernatant was decanted, the residue re-dissolved in hexane and the precipitation with MeOH was repeated three times to give analytically pure **1b** after drying *in vacuo* as a green solid. Yield 664 mg (60 %). λ_{\max} (CHCl₃)/nm 350 ($\epsilon/\text{dm}^3 \text{ mol}^{-1} \text{ cm}^{-1}$ 93 400), 649 (55 600), 668 (170 000), 705 (188 000); δ_{H} (300 MHz, 0.01 mol dm⁻³ in CDCl₃, Me₄Si, 25 °C) 9.58 (8 H, s, arom. H), 4.66 (16 H, t, *J* 7.3, CH₂O), 2.04 (16 H, quint, *J* 7.3, OCH₂CH₂), 1.20–1.67 (144 H, m, CH₂), 0.84 (24 H, t, *J* 7.0, Me), –1.65 (2 H, br s, NH); δ_{C} (75 MHz, 0.01 mol dm⁻³ in CDCl₃, Me₄Si, 25 °C) 167.5, 137.1, 134.5, 124.3, 66.7, 31.9, 29.8, 29.7, 29.7, 29.5, 29.4, 26.2, 22.7, 14.1 (2 signals of CH₂ missing due to overlap); *m/z* (MALDI) 2211.6 (M⁺).

2,3,9,10,16,17,23,24-Octakis(2-hexyldecyl-1-oxycarbonyl)-(29H, 31H)-phthalocyanine (1d).

Prepared similarly to **1c** from **3** (433 mg, 0.5 mmol) and 2-hexyl-1-decanol (**4d**) (10 mmol, 2.90 cm³) with the following amendment: the crude product was isolated by flash chromatography with CH₂Cl₂. The crude product was applied on the SiO₂ column, excess of **4d** was eluted with MeOH, and then **1d** was eluted with CH₂Cl₂. Viscous green oil. Yield 838 mg (63 %).

λ_{\max} (CHCl₃)/nm 350 ($\epsilon/\text{dm}^3 \text{ mol}^{-1} \text{ cm}^{-1}$ 97 700), 649 (55 900), 668 (175 000), 705 (194 000); δ_{H} (300 MHz, 0.01 mol dm⁻³ in CDCl₃, Me₄Si, 25 °C) 9.88 (8 H, s, arom. H), 4.52 (16 H, d, *J* 6.2, CH₂O), 2.02 (8 H, m, CHCH₂O), 1.17–1.65 (192 H, m, CH₂), 1.00 (24 H, t, *J* 7.0, Me), 0.87 (24 H, t, *J* 6.9, Me), –0.17 (2 H, br s, NH). δ_{C} (75 MHz, 0.01 mol dm⁻³ in CDCl₃, Me₄Si, 25 °C) 167.8, 137.9, 134.7, 124.6, 69.6, 37.5, 31.9, 31.4, 30.1, 29.8, 29.7, 29.4, 26.8, 26.8, 22.7, 22.6, 14.1, 14.0 (2 signals of CH₂ missing due to overlap); *m/z* (MALDI) 2660.0 (M⁺).

2,3,9,10,16,17,23,24-Octakis(2-octyl-dodecyl-1-oxycarbonyl)-(29H, 31H)-phthalocyanine (1e).

Prepared similarly to **1d** from **3** (200 mg, 0.23 mmol) and 2-octyl-1-dodecanol (**4e**) (1.44 cm³, 4 mmol). Viscous green oil. Yield 407 mg (57%).

λ_{\max} (CHCl₃)/nm 350 ($\epsilon/\text{dm}^3 \text{ mol}^{-1} \text{ cm}^{-1}$ 95 900), 649 (55 000), 668 (172 000), 705 (189 000); δ_{H} (300 MHz, 0.01 mol dm⁻³ in CDCl₃, Me₄Si, 25 °C) 9.88 (8 H, s, arom. H), 4.51 (16 H, d, *J* 6.0, CH₂O), 2.02 (8 H, m, CHCH₂O), 1.10–1.65 (256 H, m, CH₂), 0.79 (24 H, t, *J* 6.2), 0.75 (24 H, t, *J* 6.8), –0.17 (br s, 2H); δ_{C} (75 MHz, 0.01 mol dm⁻³ in CDCl₃, Me₄Si, 25 °C) 167.8, 137.9, 134.7, 124.6, 69.6, 37.5, 31.9, 31.8, 31.4, 30.1, 29.8, 29.7, 29.7, 29.4, 29.3, 26.8, 22.7, 22.6, 14.1, 14.0 (4 signals of CH₂ missing due to overlap); *m/z* (MALDI) 3108.7 (M⁺).

2,3,9,10,16,17,23,24-Octacyano-(29H, 31H)-phthalocyanine (2).

Solid state NMR: δ_{C} (75 MHz, 25 °C) 140.6 (C=N), 137.5, 126.4 (CH), 117.3, 111.3 (CN); *m/z* (FD in the presence of CuCl₂): found: *m/z* 775.04 (M⁺); C₄₀H₈CuN₁₆ requires 775.05.

2,3,9,10,16,17,23,24-Octacarboxy-(29H, 31H)-phthalocyanine (3).

δ_C (75 MHz, NaOD/D₂O, 25 °C, Me₃SiCH₂CH₂COONa as internal standard) 177.9 (COOH), 157.2, 139.1, 138.8, 120.8. m/z (MALDI) 866 (M⁺, 100), 848 ([M – H₂O]⁺, 48), 823 ([M – CO₂ + H]⁺, 43).

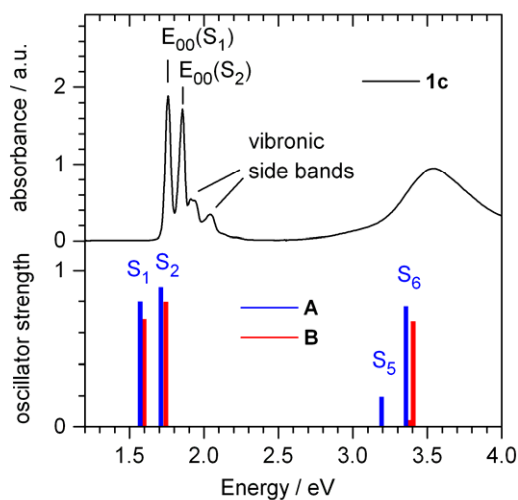


Fig. S1. Absorption spectra of phthalocyanines. Top: experimental spectrum of **1c** in CHCl₃; E₀₀(S₁) and E₀₀(S₂) are the adiabatic transition energies of the lowest electronic states; the vibronic side bands of S₁ (ca. 1.94 eV) and of S₂ (ca. 2.04 eV) are indicated. Bottom: Calculated stick spectra of the vertical electronic transition energies of **A** (blue) and **B** (red); geometry optimization: DFT B3LYP/6-31G*; electronic structure: ZINDO/S.

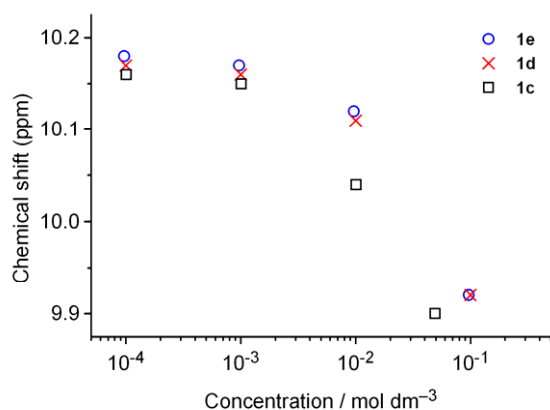


Fig. S2. Concentration-dependent ¹H chemical shifts of aromatic protons in **1c**, **1d** and **1e** recorded at 25 °C in C₆D₆.

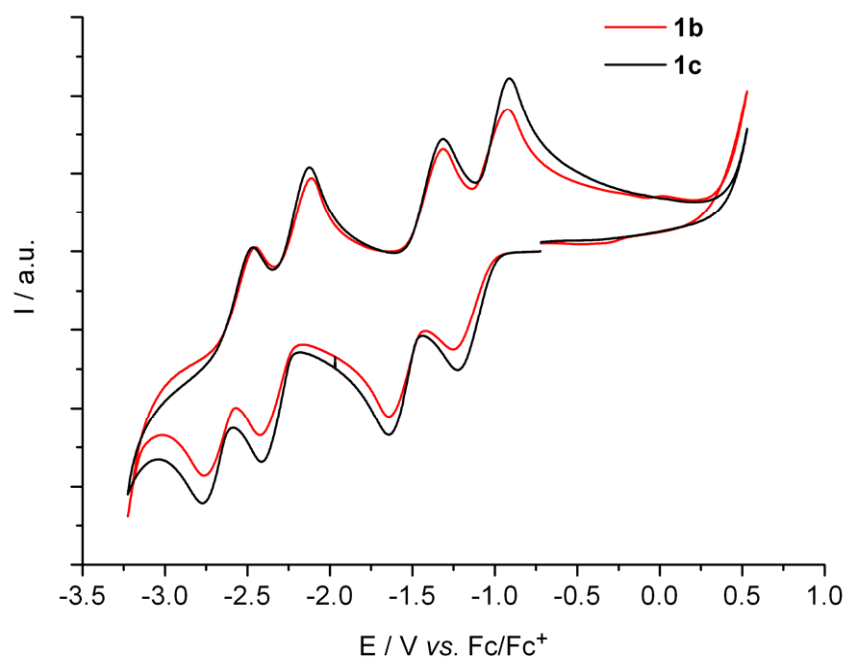


Fig. S3. CV curves of **1b** (red) and **1c** (black) in THF (10^{-3} mol dm⁻³) containing TBAPF₆ (0.1 mol dm⁻³); 25 °C, scan rate 100 mV s⁻¹; potentials vs. Fc/Fc⁺.

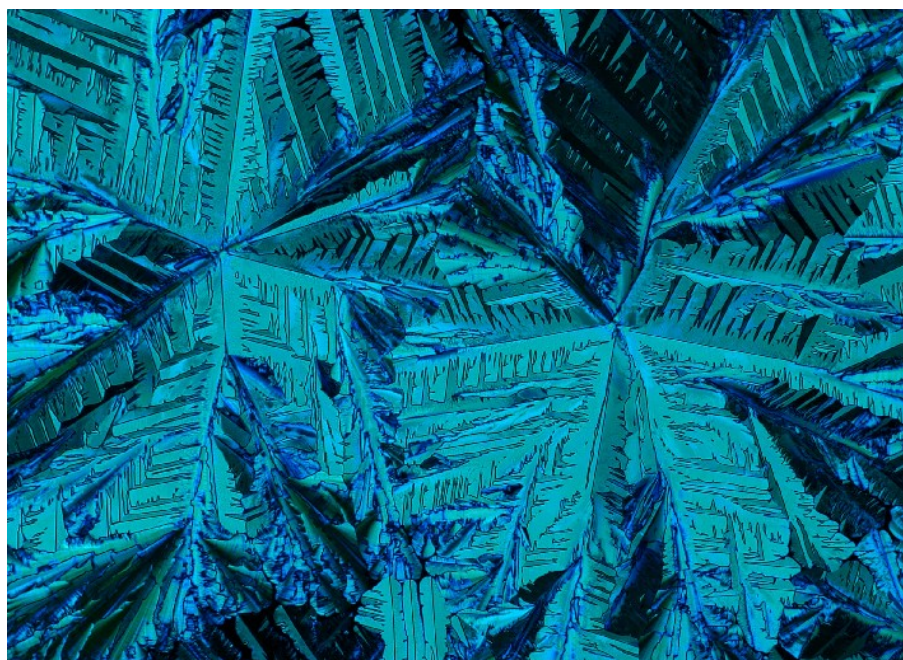


Fig. S4. Cross-polarized optical microscopy image of **1c** after cooling from isotropic liquid (160 °C) to columnar mesophase (140°C).

Table S1. Detailed indexation of liquid crystalline phase of **1c** at different temperatures.^a

1c	<i>h</i>	<i>k</i>	<i>l</i>	<i>d</i> _{calc} (Å)	<i>d</i> _{exp} (Å)	Lattice parameters ^a
Col_r at 25°C	1	1		23.7	23.7	<i>a</i> = 40.3 Å
	2	0		20.1	20.2	<i>b</i> = 29.4 Å
	1	3		9.5	9.5	<i>γ</i> = 90.0°
	0	0	1		4.5 (broad halo) No apparent reflection	<i>S</i> = 1184.8 Å ²
Col_r at 50°C	1	1		23.7	23.7	<i>a</i> = 40.2 Å
	2	0		20.1	20.1	<i>b</i> = 29.3 Å
	1	3		9.5	9.5	<i>γ</i> = 90.0°
	0	0	1		4.5 (broad halo) No apparent reflection	<i>S</i> = 1177.9 Å ²
Col_r at 100°C	1	1		23.6	23.6	<i>a</i> = 39.8 Å
	2	0		19.9	19.9	<i>b</i> = 29.3 Å
	1	3		9.5	9.5	<i>γ</i> = 90.0°
	0	0	1		4.6 (broad halo) No apparent reflection	<i>S</i> = 1166.1 Å ²
Col_r at 140°C	1	1		23.5	23.5	<i>a</i> = 39.6 Å
	2	0		19.8	19.8	<i>b</i> = 29.2 Å
	1	3		9.4	9.4	<i>γ</i> = 90.0°
	0	0	1		4.6 (broad halo) No apparent reflection	<i>S</i> = 1156.3 Å ²

^a *d*_{calc} and *d*_{exp} are the calculated and experimental diffraction spacings, respectively; *hk* is the indexation of the two-dimensional lattice (Miller indices); *a*, *b* and *γ* are the lattice parameters; *S* is the lattice area; Col_r: 2D rectangular columnar phase.

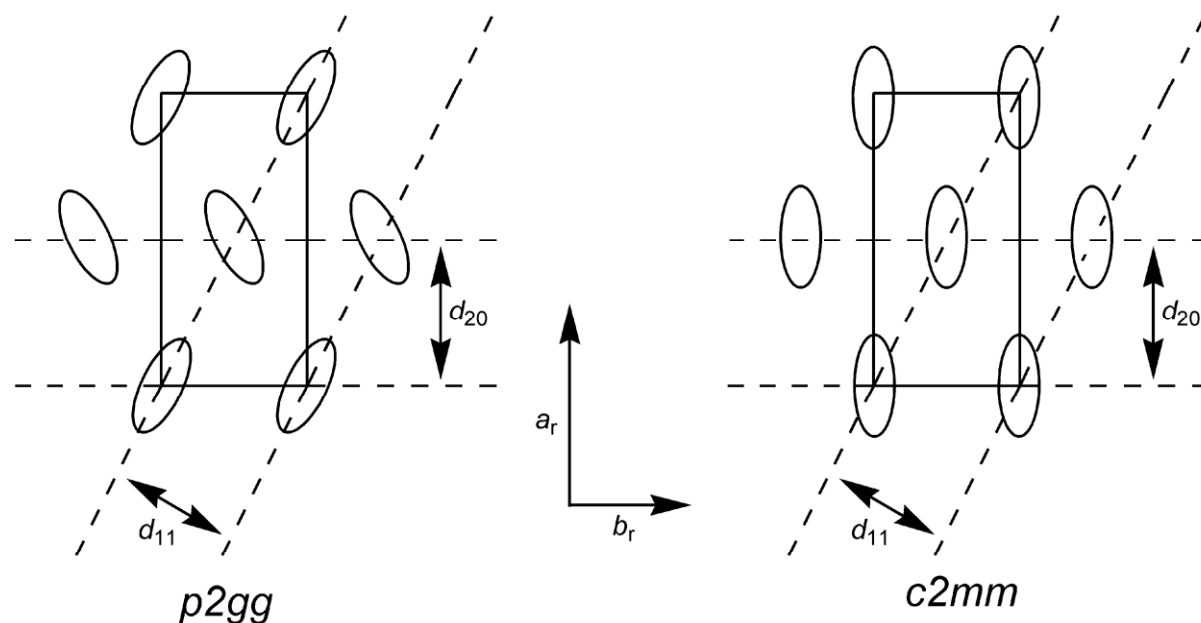


Fig. S5. Lateral structures of rectangular columnar phases and their respective plane groups (Hermann-Mauguin nomenclature)^{S1}. Schematic representation of the 2D lattices of the two rectangular columnar mesophases: with a *p2gg* plane group (left) and with a *c2mm* plane group (right).^{S2} These two arrangements include two columns per lattice and the elementary 3D cell is orthorhombic.

Solid state NMR

Instrumentation

All solid state NMR experiments were performed on a Bruker spectrometer with a ^1H frequency of 700.13 MHz and a ^{13}C frequency of 176.05 MHz. A Bruker double resonance probe supporting rotors of 2.5 mm outer diameter was used at a spinning frequency of 25 kHz for ^{13}C cross-polarization (CP) magic angle spinning (MAS) experiments. The RF precession frequencies were set to 100 kHz for both channels. The ^{13}C CP MAS measurement have been recorded with 2 s recycle delay, 1 ms CP contact time using a variable amplitude contact pulse (80–100%)^{S3} and two-pulse phase-modulation (TPPM) ^1H decoupling during the acquisition.^{S4}

At high spinning frequencies, additional heating effects caused by bearing gas friction become significant. The given sample temperature has been corrected for the frictional heating effect following the described procedure.^{S5}

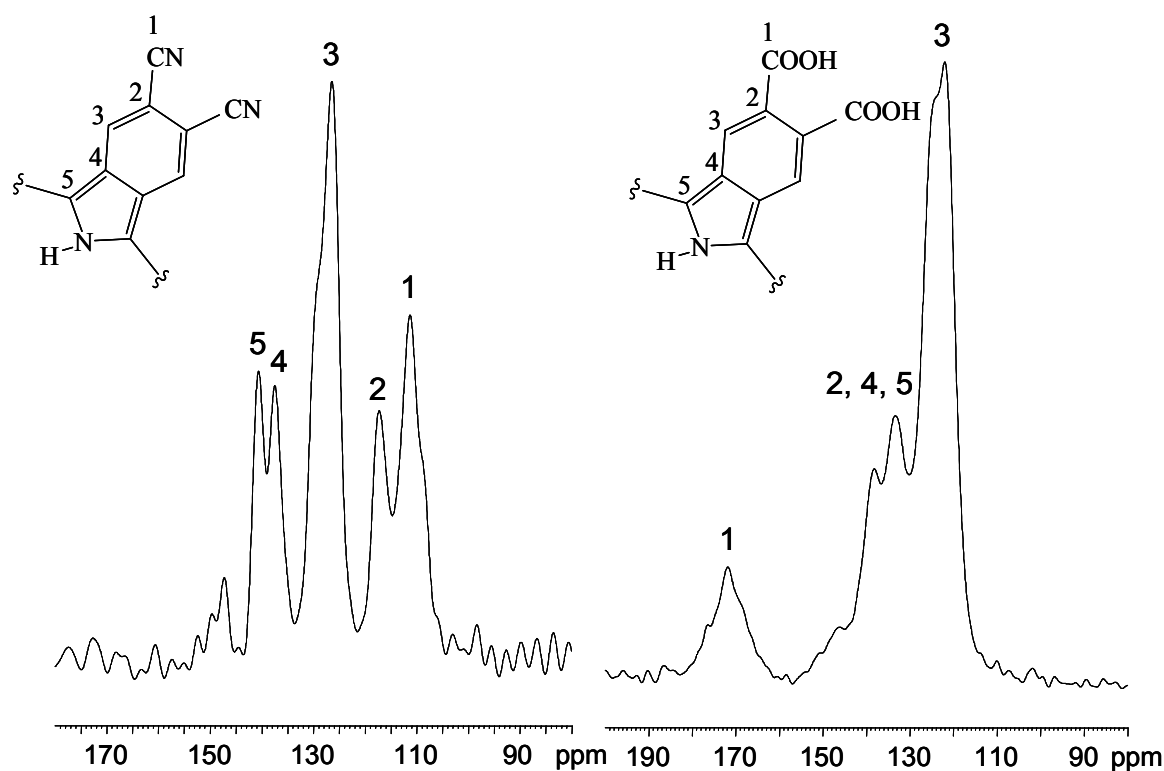


Fig. S6. ^{13}C CP MAS NMR spectra of **2** (left, 3 k transients) and **3** (right, 20 k transients) at 313 K. Due to the unfavorable distribution of the ^{13}C chemical shifts of the quaternary carbons in the case of compound **3**, the aromatic signals could not unambiguously be assigned from the CP MAS spectrum.

References

- S1 *International Tables for Crystallography, Vol. A: Space-group symmetry*, ed. T. Hahn, 5th Edition, Published for The International Union for Crystallography by Kluwer Academic Publishers Dordrecht/Boston/London, 2002.
- S2 J. W. Goodby, G. W. Gray, *Handbook of Liquid Crystals, Vol. 1: Fundamentals*, eds. D. Demus, J. Goodby, G. W. Gray, H-W. Spiess, V. Vill, Wiley-VCH Publishers, Weinheim New York, **1998**, p. 668.
- S3 G. Metz, X. Wu, S. O. Smith, *J. Magn. Res.* **1994**, *110*, 219.
- S4 A. E. Bennet, C. M. Rienstra, M. Auger, K. V. Lakshmi, R. G. Griffin, *J. Chem. Phys.* **1995**, *103*, 6951.
- S5 B. Langer, I. Schell, H. W. Spiess, A.-R. Grimmer, *J. Magn. Res.* **1999**, *138*, 182.